Evaluation of (η^5-C_5H_5)(CO)Ni–In[$(CH_2)_3N(CH_3)_2$]$_2$ as a Single-Molecule Precursor for OMCVD of Binary Ni/In Alloys. Deposition of Phase-Pure Polycrystalline ϵ-NiIn

Roland A. Fischer* and Matthias Kleine

Anorganisch-chemisches Institut, Technische Universität München, Lichtenbergstrasse 4, D-85747 Garching, Germany

Olaf Lehmann and Michael Stuke[†]

Max-Planck Institut für Biophysikalische Chemie, Abteilung Laserphysik, Am Fassberg, D-37077-Göttingen, Germany

Received March 10, 1995. Revised Manuscript Received June 12, 1995[⊗]

The volatile heterodinuclear organometallic compound (η^5-C_5H_5)(CO)Ni-In[$(CH_2)_3N(CH_3)_2$]$_2$ (**1**) has been shown to serve as a single-molecule precursor to deposit Ni/In alloy thin films by thermal chemical vapor deposition using either a horizontal hot-wall reactor in the absence of carrier gases in vacuo or a vertical cold-wall reactor with the carrier gases N_2 and H_2. The metal ratios of the thin films depend on the substrate temperature. Nickel rich films were deposited below 250 °C. The 1:1 stoichiometry of the metals of the precursor compound is perfectly retained above 350 °C. Typical growth rates were between 0.1 and 3 Å s^{-1}. At low substrate temperatures the cyclopentadienyl ligand is transferred from the nickel atom to the indium center during the film growth generating volatile and thermally stable [(η^5-C_5H_5)In] which leaves the reaction zone. Other byproducts were mainly cyclopentadiene and unsaturated dimethylpropylamines, e.g., H_2C=$CHCH_2NMe_2$. The films were examined by SEM-EDX and Auger electron spectroscopy and proved to be reasonably pure showing levels of C, O, and N below 1–2 atom % and exhibit specific resistivities in the range of 250(±50) $\mu\Omega$ cm. Films grown on various substrates (quartz, GaAs, InP) were structurally characterized by X-ray diffraction showing the hexagonal ϵ-NiIn as the only detectable crystalline phase. Plasma enhanced MOCVD experiments were also performed and expectedly showed a much lower selectivity of the decomposition chemistry of the precursor. Ni/In microstructures (e.g., squares of 200 μm side length, a line width of 25 μm and a line height of 12 μm) were drawn by photothermic laser direct writing on Al_2O_3 substrates.

Introduction

Selected binary alloys containing transition metals and aluminum, gallium, or indium have been shown to serve as epitaxial and thermodynamically stable metal III/V–semiconductor interfaces, for example, as novel Ohmic contacts or as Schottky barriers.[1–5] The fabrication of these heterostructures is currently achieved by molecular beam epitaxy. However, this technique is not generally suitable for industrial mass production of microelectronic devices.[6] Efforts undertaken to develop alternative methods to deposit such mixed metal thin films using volatile organometallic sources and CVD techniques are still limited to very few examples.[7–9] The typical approach in chemical vapor deposition of binary materials is based on individual molecular sources which carry the particular constituents of the final thin film. The composition of the coating is then controlled by the precise adjustment and optimization of the process parameters. This most importantly includes the relation of the molar fractions of the different source molecules in the gas phase at the reactor inlet, as well as the total pressure and the substrate temperature. By this strategy, rather pure and epitaxial β-CoGa was grown on (100)GaAs using (η^5-C_5H_5)$(CO)_2$Co and a considerable excess of $Ga(C_2H_5)_3$ at atmospheric pressure in the presence of hydrogen.[8] Whether or not so-called “single source precursors”, which contain all constituents of the final material in one single precursor molecule, may be equally interesting or even advantageous over separate sources in certain cases is still a matter of ongoing controversial discussion.[10–12] For

† Laser direct writing of metallic microstructures.

⊗ Abstract published in *Advance ACS Abstracts,* August 1, 1995.

(1) Williams, R. S. *Appl. Surf. Sci.* **1992**, *60/61*, 613.
(2) Tanaka, M.; Ikarashi, N.; Sakakibara, H.; Ishida, K.; Nishinaga, T. *Appl. Phys. Lett.* **1992**, *60*, 835.
(3) Baugh, D. A.; Talin, A. A.; Williams, R. S.; Kuo, T.-C.; Wang, K. L. *J. Vac. Sci. Technol.* **1991**, *B9*, 2154.
(4) Kuo, T. C.; Wang, K. L.; Arghvani, R.; George, T.; Lin, T. L. *J. Vac. Sci. Technol.* **1992**, *B10*, 1923.
(5) Kuo, T. C.; Kang, T. W.; Wang, K. L. *J. Cryst. Growth* **1991**, *111*, 996.
(6) Chow, P. P. In *Thin Film Processes II*, Vossen, J. L., Kern, W., Eds.; Academic Press: San Diego, 1991; p 133.
(7) Maury, F.; Brandt, L.; Kaesz, H. D. *J. Organomet. Chem.* **1993**, *449*, 159.
(8) Maury, F.; Talin, A. A.; Kaesz, H. D.; Williams, R. S. *Chem. Mater.* **1993**, *5*, 84.
(9) (a) Chen, Y.; Kaesz, H. D.; Kim, Y. K.; Müller, H. J.; Williams, R. S.; Xue, Z. *Appl. Phys. Lett.* **1989**, *55*, 2760. (b) Kaesz, H. D.; Williams, R. S.; Hicks, R. F.; Zink, J. I.; Chen, Y.-J.; Müller, H.-J.; Xue, Z.; Xu, D.; Shuh, D. K.; Kim, Y. Y. *New J. Chem.* **1990**, *14*, 527.
(10) (a) Aylett, B. J.; Colquhoun, H. M. *J. Chem. Soc., Dalton Trans.* **1977**, 2058. (b) Aylett, B. J.; Colquhoun, H. J. *J. Chem. Soc., Dalton Trans.* **1977**, 2058. (c) Aylett, B. J.; Tannahill, A. A. *Vacuum* **1985**, *35*, 435.

0897-4756/95/2807-1863$09.00/0 © 1995 American Chemical Society

metal oxides, nitrides, and carbides, which altogether represent metal/nonmetal combinations, it seems that single sources now attract growing interest by the manufacturers. Well-known examples include the TEOS process,[13] TiN from $(R_2N)_4Ti$ precursors,[14-16] BSG from $B(OSiR_3)_3$,[17] and recently GaN from $[R_2GaN_3]_3$ type precursors.[18] However, in the case of classical metallic alloys, e.g., Hume Rothery phases or Laves phases, very few systematic studies on single sources have been undertaken so far.[9,19] Ayletts's work on the deposition of transition metal silicides from organometallic silicon compounds may be regarded as one important exception counting the semimetal silicon as a metal.[10] Recently we reported on the design of organometallic mixed metal complexes of the type $L(CO)_nM-ER_2(Do)$ (M = d-block metal; E = Al, Ga, In; R = alkyl, L = CO, PR_3, Cp; Do = O, N Lewis base donor) and we were able to demonstrate that these systems serve as precursors for low pressure MOCVD of the corresponding phase pure intermetallic thin films M_1E_{1-x} ($0 \leq x \leq 0.5$), e.g., β-CoGa or ϵ-NiIn.[20-22] Since then, a number of manuscripts have been published describing transition-metal group 13 metal chemistry and stressing its potential importance for the deposition of mixed metal thin films.[23-26] The heterodinuclear complex $(\eta^5\text{-}C_5H_5)(CO)NiIn[(CH_2)_3N(CH_3)_2]_2$ (**1**) represents the first and still only organoindium compound known to date, which also contains the metal nickel (Figure 1). Compound **1** was specifically synthesized to serve as a single source precursor for MOCVD applications. It had been conjectured, that the ϵ-NiIn phase may be qualified as a stable metal contact to III/V-semiconductors, and in particular as an Ohmic contact for InP.[9b] Here we report in detail on the evaluation of **1** to deposit Ni/In alloys and phase-pure stoichiometric ϵ-NiIn films.

Experimental Section

Precursor Preparation, Characterization, and Handling. All manipulations were carried out under dry and oxygen-free nitrogen or argon atmosphere using oven-dried glassware. Solvents were freshly distilled from Na/K alloy. The synthesis of $(\eta^5\text{-}C_5H_5)(CO)NiIn[(CH_2)_3N(CH_3)_2]_2$ (**1**) from $[(\eta^5\text{-}C_5H_5)(CO)Ni](K)$[27] and $BrIn[(CH_2)_3N(CH_3)_2]_2$[28] on a typical scale of 10–20 mmol (5–10 g) has been described in detail elsewhere[29] (Figure 1). The compound sublimes quantitatively without decomposition at 80–90 °C and 10^{-3} Torr at practical rates up to 1–2 g h^{-1}. All manipulations with the precursor compound **1** should be conducted by a skilled person using inert-gas techniques and a closed apparatus (e.g., Schlenk-line or glove box) in combination with a well-ventilated hood. Due to the significant volatility of the compound, and its partial hydrolysis into volatile $[(\eta^5\text{-}C_5H_5)(CO)Ni-H]$ and $(HO)\text{-}In[(CH_2)_3N(CH_3)_2]_2$ in air, which both compounds may exhibit a significant toxicity, care must be taken to avoid any inhalation. The compound is not pyrophoric and can be stored under inert-gas atmosphere with cooling (−10 °C) for an unlimited period of time. Any residue of the precursor **1** can be safely destroyed either by careful oxidative acid hydrolysis with diluted H_2O_2/H_2SO_4 with cooling or by dissolution into 2-propanol/KOH.

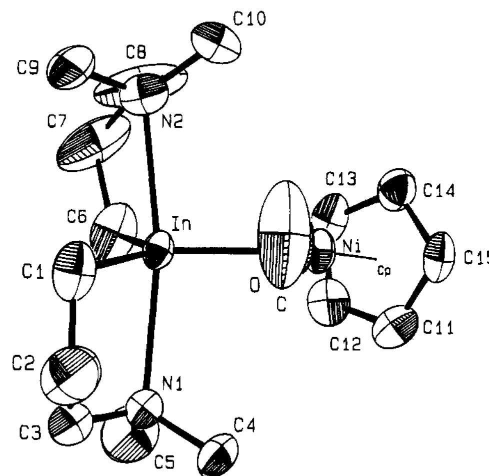

Figure 1. Molecular structure of $(\eta^5\text{-}C_5H_5)(CO)Ni-In[(CH_2)_3N\text{-}(CH_3)_2]_2$ in the crystal (ORTEP drawing, with thermal ellipsoids drawn at a 50% level).[29]

NMR spectra were recorded using a JEOL GMX 400 spectrometer (C_6D_6, 20 °C). Elemental analysis were obtained from the Microanalytic Laboratory of the Technical University Munich. Mass spectra were recorded on Finnigan MAT 90 (EI, 70 eV) and Varian MAT 311a (FI and CI with isobutene) spectrometers. Gas chromatographic analyses were performed using a HP 5890 equipped with a mass selective detector system (HP 5970B). A fused silica capillary column (HP-1, 19091Z-102, with 100% methylpolysiloxane (l = 50 m, o.d. = 0.2 mm, film thickness = 0.33 μm) was used.

Film Deposition by MOCVD. The vacuum MOCVD experiments were carried out in an isothermal horizontal hot-wall quartz tube reactor shown in Figure 2a. The substrates for CVD studies consisted of borosilicate microscope slides, quartz, (111)silicon slides (100)InP and (100)GaAs slides, which were cleaned by degreasing in trichloroethylene, washing with 2-propanol/acetone and rinsing in deionized water and by usual etching procedures. After loading the reactor with various substrates the system was evacuated to a base pressure of $<10^{-6}$ Torr. The precursor reservoir was loaded under an inert gas atmosphere with 1–2 g of the precursor compound and cooled to −30 °C and the valve to the reactor was opened. The system was evacuated again to 10^{-6} Torr for several hours, while the temperature of the furnace was set at the desired value and was allowed to stabilize. The temperature profile of the furnace was measured showing a maximum negative deviation of 30–50 °C from the temperature at the center (200–400 °C). The temperature of the precursor reservoir was then adjusted between 50 and 90 °C and the precursor was sublimed through the hot zone at pressures of 10^{-1}–10^{-4} Torr, giving reflective metallic depositions on the wall of the tube and on the substrates. Carrier gases were not used in these experiments.

The low-pressure plasma enhanced MOCVD experiments were conducted with a standard vertical parallel plate reactor

(11) Senzaki, Y.; Gladfelter, W. *Polyhedron* **1994**, *13*, 1159.
(12) Maury, F. *Adv. Mater.* **1991**, *3*, 542.
(13) Becker, F. S.; Pawlik, D.; Anzinger, H.; Spitzer, A. *J. Vac. Sci. Technol.* **1987**, *B5*, 1555.
(14) Weber, A.; Nikulski, R.; Klages, C.-P. *Appl. Phys. Lett.* **1993**, *63*, 325.
(15) Hoffman, D. M. *Polyhedron* **1994**, *13*, 1169.
(16) Dubois, L. H. *Polyhedron* **1994**, *13*, 13296.
(17) Treichel, H.; Spindler, O.; Kruck, T. *J. Phys.* **1988**, *49*, C4.
(18) Kouvetakis, J.; Beach, D. *Chem. Mater.* **1989**, *1*, 476.
(19) Hampden-Smith, M. J.; Kodas, T. T. In *The Chemistry of Metal CVD*; Verlag Chemie: Weinheim, 1994; Chapter 8, pp 414–415.
(20) Fischer, R. A.; Scherer, W.; Kleine, M. *Angew. Chem., Int. Ed. Engl.* **1993**, *32*, 748.
(21) Fischer, R. A.; Behm, J.; Priermeier, T.; Scherer, W. *Angew. Chem., Int. Ed. Engl.* **1993**, *32*, 746.
(22) Fischer, R. A. In *Mater. Res. Soc. Symp. Proc.*; Abernathy, C. R., Bates, J. C. W., Bohling, D. A., Hobson, W. S., Eds.; Materials Research Society: Pittsburgh, PA, 1993; pp 267–273.
(23) Cowley, A. H.; Gabbai, F. P.; Decken, A. *Angew. Chem., Int. Ed. Engl.* **1994**, *33*, 1370.
(24) Cowley, A. H.; Decken, A.; Olazábal, C. A.; Norman, N. C. *Inorg. Chem.* **1994**, *33*, 3435.
(25) Olazábal, C. A.; Cowley, A. H. *Organometallics* **1994**, *13*, 421.
(26) Dohmeier, C.; Krautscheid, H.; Schnöckel, H. *Angew. Chem., Int. Ed. Engl.* **1994**, *33*, 2482.
(27) Fischer, R. A.; Behm, J.; Herdtweck, E.; Kronseder, C. *J. Organomet. Chem.* **1992**, *437*, C29.
(28) Schumann, H.; Görlitz, F. H.; Seuss, T. D.; Wassermann, W. *Chem. Ber.* **1992**, *125*, 3.
(29) Fischer, R. A.; Herdtweck, E.; Priermeier, T. *Inorg. Chem.* **1994**, *33*, 934.

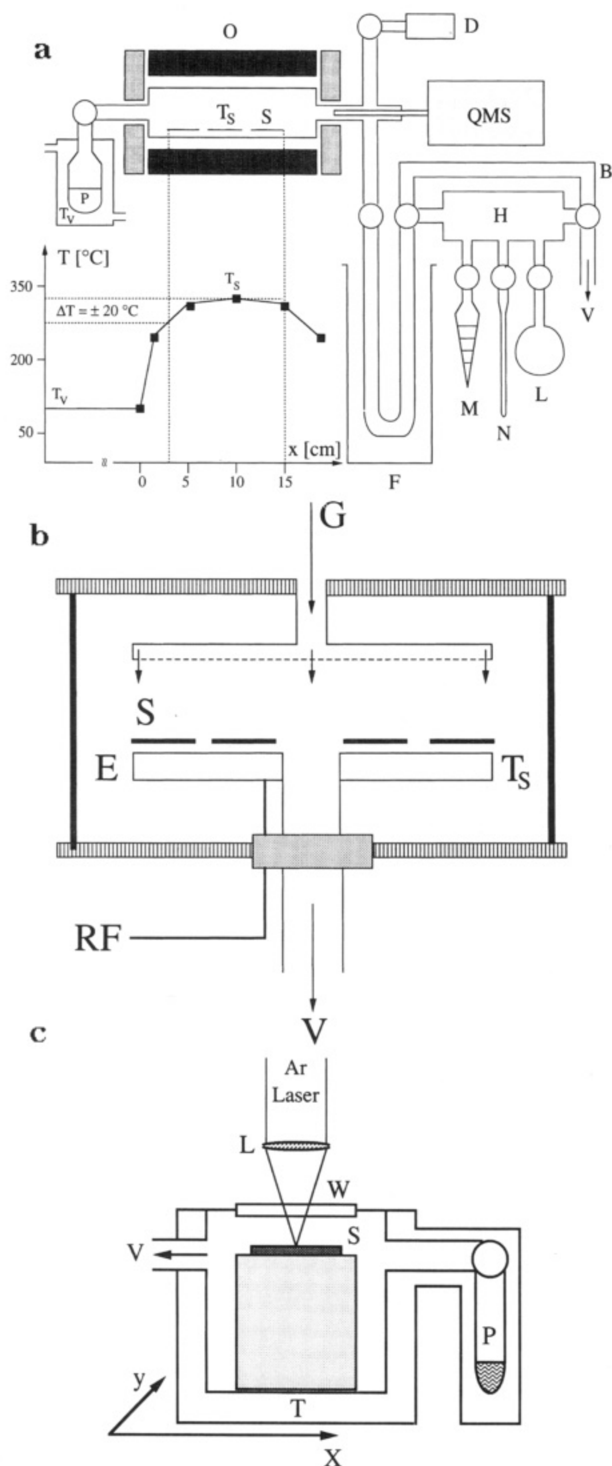

Figure 2. (a, top) Schematic drawing of the hot-wall horizontal tube reactor (O) used for the vacuum MOCVD experiments in the absence of carrier gases. A quadrupolar mass spectrometer (QMS) with a sampling unit (0.7 mm orifice) is connected to the reactor exit where the total pressure (D) is measured. The condensable parts of the volatile effluent are collected in a cold trap (F) which is attached to a high vacuum line (H; graded volume, M; NMR tube, N; NMR solvent, L). A bypass (B) connects the cold trap with the vacuum pump system (V, turbo molecular pump). The precursors were filled into the thermostated (T_v, temperature of volatilization) reservoire P. A typical temperature profile of the oven is given below. (b, middle) Schematic drawing of the vertical parallel plate cold wall reactor used for plasma-enhanced MOCVD and pure thermal CVD experiments with carrier gases. (RF: rf-generator system; G, gas inlet; E, heated rf-electrode and substrate holder; T_s, substrate temperature; V, to the vacuum system). (c, bottom) Schematic drawing of the general setup for laser direct writing of metallic microstructures. The substrates were mounted into a small vacuum chamber equipped with an optical window (W). The precursor reservoir (P) and the camber were both heated to 80−90 °C. The substrate is selectively heated using a focused laser beam (B). The whole arrangement was mounted onto a table which could be moved into two directions (x, y) by computer control.

(Figure 2b; radial flow batch type).[30,31] The substrates were mounted onto the rf electrode, which can be heated up to 350−400 °C. Traces of oxygen and water were removed to a level of <0.1 ppm for O_2 and <0.5 ppm for H_2O from the carrier gases (N_2 and H_2) using a commercial gas purification system (Oxisorb, EM-Kat, Hydrosorb, Messer Griesheim). The mass flow was adjusted by electronic mass-flow controllers (1259 CY, MKS) and the total pressure in the system was measured by a Pirani gauge (TPR 010, TPR 300; Balzers). The same reactor was used for pure thermal cold wall low pressure CVD experiments in the absence of the plasma.

"Laser direct writing" of Ni/In microstructures was performed using an apparatus sketched in Figure 2c in collaboration with Dr. M. Stuke and O. Lehmann at the Max-Planck Institute at Göttingen, Germany. The experimental setup has been described in detail elsewhere[32] and is similar to other systems which were used for example for laser direct writing of gold structures.[33] The structures were drawn at a laser power of 500 mW and a scan velocity of 50 μm s^{-1} using a argon ion laser at 488 nm. The precursor reservoir and the vacuum chamber were held at 90 °C at a pressure of 0.1 Torr.

Thin-Film Characterization. The films obtained were examined ex situ by various surface analytic tools (AES, SEM-EDX, and XPS) and X-ray powder diffraction. The metal ratio was determined independently by AAS after quantitative dissolution of representative films in aqueous nitric acid (6.5 weight %). Thick films were grown on the walls of the reaction tube, which peeled off by rapid cooling of the tube (10 °C s^{-1}). After collecting typical quantities of 50−100 mg of the deposited material by hand, classical combustion analysis was performed (C, H, and N). The compositions of the films were uniform over the plated areas of typically 3.2 cm^2 (AES mapping and profiling). The EDX-spectra were recorded using a scanning electron microscope JEOL JSM-35C equipped with an X-ray analysator system EG&G Ortec System 5000. A typical standardless program for quantitative analysis "AUTOZAP" 3.08 ("ZAF" correction) was employed. The obtained values for the Ni and In contents were found to be valid within a relative error of ±20% (comparison with AAS values). Auger electron spectra were recorded using a PHI 595 spectrometer with a base pressure of (2−4) × 10^{-9} Torr and a working pressure of (2−5) × 10^{-8} Torr with a standard cylindrical mirror analyzer (3 keV primary beam energy, 0.2 μA primary beam intensity, a maximum of 500 Å lateral resolution; rate of argon ion sputtering 300 Å s^{-1} on Ta_2O_5 for an area of 1 × 1 mm). Typical data collection time was 30 min for 1 keV scan width. The films were cleaned first by 5 min of argon ion (Ar^+, 3 keV) sputtering (5 × 5 mm area) at a pressure of 5 × 10^{-6} Torr. The quantitative analysis of the obtained spectra was based on differentiated spectra and accepted standard sensitivity factors[34−36] for C, N, O, Ni, and In. However, the calibration factor for In had to be corrected to 0.32(±2) on the basis of the AAS and EDX results while Ni was set at 0.27. The specific resistivity of the deposited metallic coatings were routinely checked by a usual commercial four point probe system (FPP-5000, Veeco). The analytical data are compiled in Table 1.

Structural Characterization.[20] The X-ray diffraction patterns were recorded on a Huber-Guinier diffractometer 653; Ge-monochromated Cu Kα (λ = 1.54056 Å) using the step scanning method with an angle of incident of 6°, a scan width of 0.005° (counting time of 10 s) and a rotating probe head.

(30) Reif, R. In *Thin Film Processes II*; Vossen, J. L., Kern, W., Eds.; Academic Press: San Diego, 1991; pp 523−535.

(31) Kleine, M. Ph.D. Thesis, Techn. Univ. Muenchen, 1994.

(32) (a) Gottsleben, O.; Stuke, M. *Appl. Phys. Lett.* **1988**, *52*, 2230. (b) Lehmann, O.; Stuke, M. *Appl. Phys. A* **1991**, *53*, 343. (c) Foulon, F.; Lehmann, O.; Stuke, M. *Appl. Surf. Sci.* **1993**, *69*, 87.

(33) Davidson, J. L.; John, P.; Roberts, P. G.; Jubber, M. G.; Wilson, J. I. B. *Chem. Mater.* **1994**, *6*, 1712.

(34) Davis, L. E.; McDonald, N. C.; Palmberg, P. W.; Riach, G. E.; Weber, R. E. *Handbook of Auger Elektron Spectroscopy*, 2nd ed.; Physical Electronics Inc.: Eden Prairie, MN, 1976.

(35) McGuire, G. E. *Auger Electron Spectroscopy Reference Manual*; Plenum Press: New York, 1979.

(36) Sekine, T.; Nagasawa, M. K.; Sakai, Y.; Parkes, A. S.; Geller, J. D.; Mogami, A.; Hirata, K. *Handbook of AUGER Electron Spectroscopy*; JEOL: Tokyo, 1982.

Table 1

(a) Deposition Conditions for the Vacuum MOCVD Experiments Using the Apparatus of Figure 2a (Isothermal Conditions Without Carrier Gases) and Selected Results of the Chemical Thin-Film Analysis (AAS, AES; Entries Marked with an Asterisk Were Obtained by Combustion Analysis). Symbols in Parentheses behind the Film Number Correspond to the Entries of Figure 3a

	T_s [°C]							
substrate film	200 #1 (*)	200 #3 (☆)	250 #9 (*)	300 #8 (*)	300 #2 (☆)	350 #4 (*)	350 #6 (□)	400 #5 (*)
p [Torr] (±20%)	10^{-3}	10^{-4}	10^{-3}	10^{-3}	10^{-4}	10^{-3}	10^{-2}	10^{-3}
gas flow [sccm]								
source temp T_v [°C] (±5)	80	50	80	80	50	80	100	80
deposition time [h]	12	24	6	3	6	6	2	4.5
Ni [μg] (AAS) (±5)	1094	1360	739	850	303	465	1630	362
In [μg] (AAS) (±5)	740	974	635	1050	473	862	2852	744
coated area [cm²] (±0.4)	3.2	3.2	3.2	3.2	3.2	0.38	3.2	0.42
growth rate [mg cm^{-2} h^{-1}]	0.05	0.03	0.08	0.20	0.04	0.60	0.70	0.60
growth rate [Å s^{-1}]	0.2	0.1	0.3	0.7	0.1	1.9	2.5	2.0
Ni/In (AAS)	2.9	2.7	2.3	1.6	1.3	1.1	1.1	1.0
Ni_1In_{1-x}: *x*	0.66	0.63	0.57	0.38	0.23	0.09	0.09	0.0
Ni [at. %]			58(2)		50(1)*	50(1)*		51(2)
In [at. %]			30(2)		40(1)*	46(1)*		49(2)
C [at. %]			9(1)		6(1)*	3(1)*		≪1
H [at. %]					2(1)*	1(1)*		
C/H					3*	3*		
O [at. %]			1(1)		2(1)*	<1*		≪1
N [at. %]			≪1					≪1

(b) Deposition Conditions for the Thermal Low-Pressure MOCVD Experiments Using the Apparatus of Figure 2b (with Carrier Gases, but without Plasma) and the Results of the Chemical Thin-Film Analysis (AAS, AES). Symbols in Parentheses behind the Film Number Correspond to the Entries of Figure 3a

	T_s [°C]							
substrate film[a]	250 #49 (◆)	250 #50 (◆)	300 #17 (◆)	300 #16 (◆)	350 #47 (◆)	350 #48 (◆)	250 #33 (●)	350 #25 (●)
p [Torr] (±20%)	0.1	0.1	0.1	0.1	0.1	0.1	0.1	0.1
gas flow [sccm]	10(N_2)	10(N_2)	10(N_2)	10(N_2)	10(N_2)	10(N_2)	10(H_2)	10(H_2)
source temp T_v [°C] (±5)	100	100	100	100	100	100	100	100
deposition time [h]	24	24	24	24	24	48	24	24
Ni [μg] (AAS) (±40)	558	739	444	548	763	1684	761	810
In [μg] (AAS) (±40)	413	635	562	906	1585	3203	674	1220
coated area [cm²] (±0.1)	1.1	1.1	1.1	1.1	1.1	1.1	1.1	1.1
growth rate [mg cm^{-2} h^{-1}]	0.04	0.06	0.04	0.06	0.1	0.1	0.05	0.08
growth rate [Å s^{-1}]	0.1	0.2	0.1	0.2	0.4	0.4	0.2	0.3
Ni/In (AAS)	2.6	2.3	1.5	1.2	1.0	1.0	2.2	1.3
Ni_1In_{1-x}: *x*	0.62	0.57	0.33	0.17	0.0	0.0	0.55	0.23
Ni [at. %]		58(2)		51(2)		52(2)		54(2)
In [at. %]		30(2)		49(2)		48(2)		46(2)
C [at. %]		9(1)		≪1		≪1		≪1
H [at. %]								
C/H								
O [at. %]		1(1)		≪1		≪1		≪1
N [at. %]		≪1		≪1		≪1		≪1

[a] The analytical data are averaged over 17 small substrates of equal areas.

The measured θ values are calibrated against internal polycrystalline Si powder. The results of a typical measurement on an ε-NiIn film deposited on GaAs(100) at 350 °C and 10^{-2} Torr are compiled in Table 2. Crystal system: hexagonal, space group *P6/mmm* (Int. Tab. Nr. 191); lattice parameters: $a = 524.37(5)$, $c = 435.09(5)$ pm, $c/a = 0.829$, $V = 103 \times 10^6$ pm³; molecular weight, density: 173.5 amu, 8.3 g cm^{-1}. Atom coordinates: Ni in 3 (f), $^1/_2$ 0 0; In in 1 (a), 0 0 0 and 2 (d) $^1/_3$ $^2/_3$ $^1/_2$. Film 4 of Table 1a, which was used for the presented XRD results, was grown on a GaAs slide of the dimensions 0.62(±0.02) × 0.62(±0.02) cm, area = 0.38(±0.05) cm². The film thickness was measured by profilometry (4.3(±0.2) μm) and confirmed by SEM (cross section) and sputtering. Afterward, the metal content was analyzed by AAS after dissolution of the film. The density of the film was then calculated to 8.1(±0.9) g cm^{-3}.

Byproduct Analysis. The exhaust gases of the vacuum MOCVD experiments using the horizontal reactor shown in Figure 2a were monitored by a quadrupolar mass spectrometer (gas analysis system HPR30-HAL/3F, 1–510 amu; Hiden) which was connected to the apparatus by a gas sampling unit with a pinhole (o.d. = 0.7 mm). The condensables were collected in the cold trap attached to the reactor chamber. After the deposition experiment was completed, the cold trap was isolated from the remaining apparatus and the contents were quantitatively vacuum-transferred into an NMR tube. C_6D_6 was added and the NMR tube was flame sealed. The tube contents were analyzed by ^1H and ^{13}C NMR spectroscopy. Subsequently the NMR tube was broken and the contents were characterized by a GC-MS analysis system. The results of a typical experiment (no. 4 of Table 1a) are reported as follows. The predominant species ($\Sigma > 95$ mol %) of the collected condensable effluent were identified as $H_2C{=}CHCH_2N(CH_3)_3$ ($m/z = 85$), *cis/trans*-$CH_3CH{=}CHN(CH_3)_3$ ($m/z = 85$), $CH_3CH_2CH_2N(CH_3)_3$ ($m/z = 87$), C_5H_6 (cyclopentadiene; $m/z = 66$), $C_{10}H_{17}N$ (presumably a Diels–Alder addition product of cyclopentadiene with 3,3-dimethylaminopropene; $m/z = 151$) and $C_{10}H_{12}$ (dicyclopentadiene; $m/z = 132$) with the approximate ratios of 46:18:12:18:5:1. The ratio of unsaturated to saturated amines was calculated to 5.3:1. In the case of typical low temperature vacuum MOCVD experiments, e.g., nos. 1 and 3 of Table 1a, the condensables were fractionally condensed from the cold trap at 0 °C. Using this procedure, an off-white less volatile residue was found to be left. This residue was sublimed into a small Schlenk tube at 50 °C and 10^{-3} Torr and was identified as $(\eta^5\text{-}C_5H_5)In$ by mass spectroscopy ($m/z = 180$), NMR and elemental analysis. The metal content of the condensables was measured in various experiments after

Table 2. Observed and Calculated d Values of ϵ-NiIn Deposited on GaAs (Film 4 of Table 1a)

h	k	l	rel int	d_{obs}[a]	d_{calc}[b]	$2\theta_{obs}$[a]	$2\theta_{calc}$[b]	diff
1	0	1	100	3.1352	3.1429	28.44	28.38	0.061
1	1	0	7	2.6209	2.6232	34.18	34.16	0.018
1	1	1	6	2.2468	2.2462	40.10	40.12	−0.018
0	0	2	11	2.1749	2.1761	41.48	41.47	0.009
2	0	1	18	2.0133	2.0137	44.99	44.99	−0.003
1	1	2	5	1.6745	1.6747	54.77	54.78	−0.008
2	1	1	2	1.5971	1.5972	57.67	57.68	−0.010
2	0	2	1	1.5725	1.5714	58.66	58.72	−0.066
3	0	0	1	1.5139	1.5144	61.17	61.16	0.003
3	0	1	1	1.4295	1.4302	65.21	65.19	0.016
1	0	3	1	1.3815	1.3819	67.77	67.77	0.002
2	2	0	1	1.3109	1.3114	71.97	71.96	0.011
1	1	3	1	1.2689	1.2693	74.75	74.74	0.013
2	0	3	2	1.2222	1.2225	78.13	78.13	0.004
2	2	2	1	1.1228	1.1232	86.63	86.62	0.007
3	1	3	0.5	0.9510	0.9512	108.18	108.18	0.005
4	1	2	1	0.9019	0.9022	117.31	117.30	0.005
4	0	3	1	0.8940	0.8942	118.99	118.98	0.011
4	2	1	2	0.8421	0.8423	132.31	132.32	0.010
2	2	4	1	0.8371	0.8373	133.88	133.89	−0.010

[a] Deposited ϵ-NiIn-phase (θ correction by an internal Si standard). [b] Calculated with hexagonal lattice parameters: a = 524.37(5), c = 435.09(5) pm.

aqueous work up (hydrolysis with HNO_3, 6.5 wt %) using AAS showing typical values of Ni:In ≤ 10^{-2} for substrate temperatures below 250 °C.

Results and Discussion

A series of thermal MOCVD experiments was conducted on **1** using the horizontal hot-wall vacuum CVD reactor (Figure 2a) *without* carrier gases and a vertical cold-wall low-pressure CVD reactor (Figure 2b) with either H_2 or N_2 as the carrier gas. This latter reactor was also used for plasma enhanced CVD experiments with the same carrier gases as a mixture. Typical results of the thin film analysis are summarized in Table 1.

A. Thermal MOCVD Experiments. *Ni/In Ratio in the Films, Formation of (η^5-C_5H_5)In and Byproduct Analysis.* The metal ratio of the precursor compound is not necessarily reproduced in the thin films. The temperature dependence of the Ni/In ratio of the films grown under various conditions, is shown in Figure 3a.

(a) Isothermal Vacuum Hot-Wall Conditions. The corresponding fraction of conversion of **1** into metallic depositions and gaseous byproducts as a function of the substrate temperature is shown in Figure 3b. From the pyrolysis curve an apparent activation energy of 13 (±2) kcal/mol was calculated for the decomposition process. From the temperature dependence of the growth rate (Table 1a) a similar value of 10 (±2) kcal/mol was derived. These values are considerably lower compared to the In−C bond dissociation energy of simple indium alkyls, e.g., $In(CH_3)_3$ with 54 kcal/mol.[37] They rather compare to $Ni(CO)_4$ exhibiting a Ni−CO dissociation energy of about 12 kcal/mol.[38] At low substrate temperatures (200−250 °C) and low decomposition fractions the obtained thin films are Ni rich. At higher substrate temperatures ≥350 °C and nearly quantitative conversion of the delivered precursor the Ni/In value goes down to the limiting value of one. Then, the metal ratio of the precursor compound is almost perfectly retained

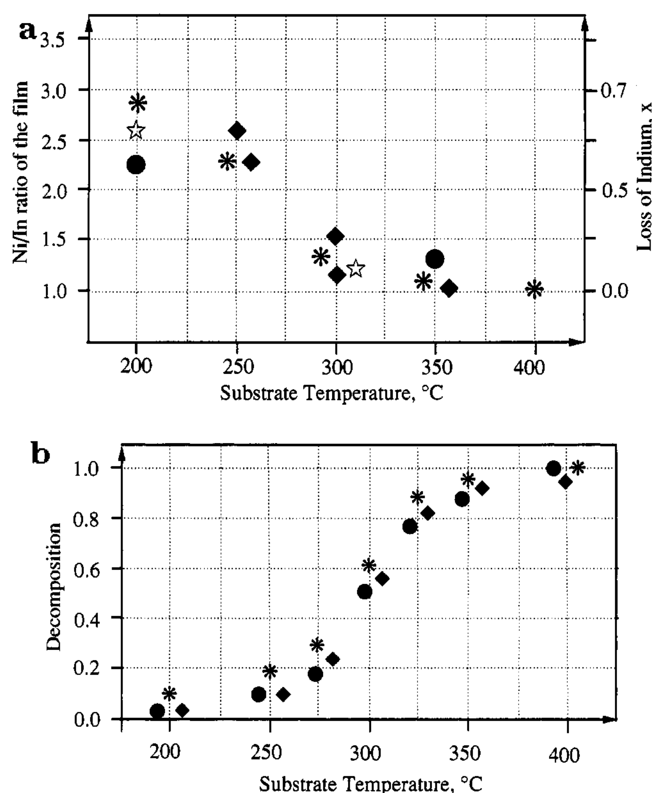

Figure 3. (a, top) Ni-to-In ratio of the obtained films Ni_1In_{1-x} and the mole fraction x of In which is lost during the deposition as a function of the substrate temperature and the conditions. (★) $p = 10^{-2}$ Torr, source temperature 80 °C; film 1, 4, 5, 8, 9 (Table 1a). (☆) $p = 10^{-4}$ Torr, source temperature 50 °C; film 2, 3 (Table 1a). (◆) $p = 10^{-1}$ Torr, source temperature 100 °C, N_2; film 16, 17, 47, 48, 49, 50 (Table 1b). (●) $p = 10^{-1}$ Torr, source temperature 100 °C, H_2; film 25, 33 (Table 1b). (b, bottom) Fraction of conversion of the delivered precursor as a function of the substrate temperature using the apparatus of Figure 2a at a constant source temperature of 80 (±2) °C and a total pressure at the reactor exit between 1 × 10^{-4} and 3 × 10^{-3} Torr. The partial pressures of characteristic fragment species are shown as fractions of their maximum (and constant) level above 400 °C. (★) [CO^+]; (●) [$H_2C{=}NMe_2^+$]; (◆) [$C_5H_6^+$].

in the films. The analysis of the effluent showed the presence of (η^5-C_5H_5)In (m/z = 180) as the only indium-containing species and H_2, CO, C_5H_6 and $H_2C{=}CHCH_2$-NMe_2 as well as isomers of this as the characteristic byproducts of the decomposition process. A typical mass spectrum of the exhaust gases is shown in Figure 4. The important fact is, that the mass spectra (EI, 70 eV) of the pure precursor compound do not show (η^5-C_5H_5)In or saturated amines such as $H_2C{=}CHCH_2NMe_2$.[29] The variation of the sublimation rate over roughly 1 order of magnitude (accompanied by the variation of the total pressure over roughly 2 orders of magnitude) had no influence on the temperature dependence of the Ni/In ratio (Figure 3a).

According to TGA-MS and DSC analysis between 25 and 100 °C compound **1** volatilizes without a significant change in the composition over long times. Only traces of decomposition products, e.g., (η^5-C_5H_5)In could be detected. Decomposition of **1** occurred at 190−200 °C. The thermal stability of (η^5-C_5H_5)In is remarkable. In an H_2 atmosphere, (η^5-C_5H_5)In pyrolyzes above 500 °C only, while no decomposition was observed in vacuo at 300−350 °C.[39] The loss of indium was almost independent from the rate of precursor delivery (sublimation

(37) Buchan, N. I.; Larson, C. A.; Stringfellow, G. B. *J. Cryst. Growth* **1988**, *92*, 247.
(38) Auvert, G. *Appl. Surf. Sci.* **1989**, *43*, 47.

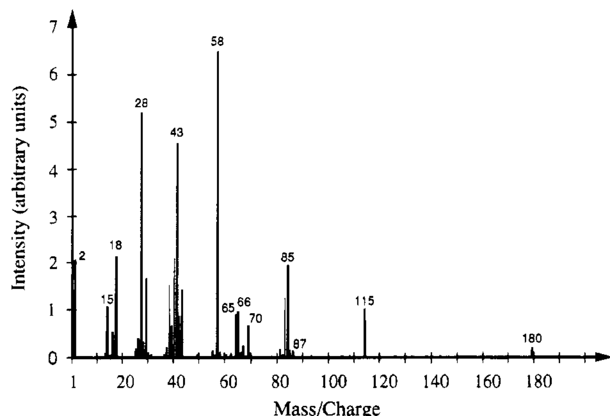

Figure 4. Typical mass spectrum of the exhaust gases at the reactor exit (Figure 2a). The spectrum is not corrected to the background (the minimum signal to background noise ratio was ~10 for $m/z = 28$). The given assignment of typical species is also based on the analysis of the condensables: m/z = 2, H_2; 66, C_5H_6; 70 , C_5H_{10}; 85, $H_2C{=}CHCH_2NMe_2$ (and isomers of this); 87, $CH_3CH_2CH_2NMe_2$; 180, $[(\eta^5\text{-}C_5H_5)In]$. The most intense fragment at m/z = 58 is due to $[H_2C{=}NMe_2^+]$ and results from the fragmentation of the (dimethylamino)amines caused by the ionization in the mass spectrometer.

rate), which was controlled by the temperature of the precursor reservoir (Table 1a, Figure 3a). Above 350 °C the growth rate was independent of the substrate temperature but an increase of the source temperature from 50 to 100 °C gave increased growth rates (Table 1a,b). Since the delivered precursor was almost quantitatively consumed above 350 °C the growth rate appears to be limited by the feeding rate of the precursor under those conditions.

The question whether homogeneous prereactions or heterogeneous surface reactions or both are responsible for the transfer of the cyclopentadienyl ligand from the nickel atom to the indium center cannot be conclusively answered at the moment. For other organometallic systems however, comparable ligand-transfer processes have been shown to occur on the native surface. The growth of copper films from (β-diketonato)Cu^IL precursors (L = PR_3, $H_2C{=}CHSiMe_3$, etc.) involves the formation of $(\beta\text{-diketonato})_2Cu^{II}$ in the course of a related ligand migration at the copper surface.[40] Another type of rearrangement is important for the deposition of pure aluminum films from the precursor $(Me_3N)Al(H)_2(\mu^2\text{-}BH_4)$ reported by Spencer et al.[41] The transfer of the amine ligand from the aluminum to the boron center leads to the liberation of thermally stable H_3BNMe_3. A similar reaction chemistry was observed during MOCVD of FeGa and FeAl thin films from $(\eta^5\text{-}C_5H_5)(CO)_2Fe{-}E[(CH_2)_3NMe_2](\eta^2\text{-}BH_4)$ (E = Al, Ga).[42,43] The alkylborane $H_2B[(CH_2)_3NMe_3]$ was identified in the effluent.[44] The migration of a cyclopentadienyl group in the condensed phase (melt or solution) has been reported in the literature. A good discussion of this effect with respect to the precursor design was given by Steigerwald in connection with the bulk pyrolysis of $[(\eta^5\text{-}C_5H_5)(CO)_2Fe]_2Te_x$ (x = 1, 2). During this pyrolysis ferrocene was removed by sublimation and $FeTe_x$ was formed.[45,46] In view of molecular chemistry the iron compound $(\eta^5\text{-}C_5H_5)(CO)_2Fe\text{-}In[(CH_2)_3NMe_2]_2$ (**2**)[21] is a very close analogue to the Ni−In system **1**. The Fe−In compound **2** can formally be derived from **1** by replacing the Ni atom of **1** with the isoelectronic Fe−CO group. However, **2** behaves strikingly different from **1** during low pressure MOCVD. An experiment with two heating zones in line was conducted. Indium rich films, e.g., $Fe_{0.6}In_1$, were deposited in the first and cold zone (T = 250 °C). Fe-rich films were deposited in the second and hot zone (T = 500 °C). In thise case, ferrocene rather than $(\eta^5\text{-}C_5H_5)In$ was formed during the low-temperature pyrolysis (first zone). Similar observations were made for the compound $[(\eta^5\text{-}C_5H_5)(CO)_2Fe]_3In$ which also gave In-enriched deposits.[47] The standard enthalpy of formation of nickelocene of 357.7 kJ mol^{-1} is significantly greater than that of ferrocene, which amounts 241.4 kJ mol^{-1}.[48] The average bond dissociation energy D(M−Cp) for nickelocene (247 kJ mol^{-1}) is somewhat lower compared to the value of 297 kJ mol^{-1} for ferrocene. The standard enthalpy of the formation of the M/In phases are exothermic but comparably small in the range of 10−30 kJ/mol^{-1}.[49] These values may support the conjecture that the decomposition reactions of the precursors **1** and **2** are controlled by chemical kinetics rather than by thermodynamics. This view is also supported by the behaviour of the related cobalt compound $(CO)_4Co\text{-}In[(CH_2)_3NMe_2]_2$ (**3**)[21,29] which does not contain a cyclopentadienyl ligand. Consequently, **3** does not show any temperature dependence of the Co/In ratio of the obtained thin films grown at temperatures as low as 200 °C, although a phase with the nominal composition Co_1In_1 is thermodynamically unstable.[50] Scheme 1 summarizes the chemistry of the decomposition of the related precursors $L(CO)_nM\text{-}In[(CH_2)_3NMe_2]_2$ (**1**−**3**: L = CO, $\eta^5\text{-}C_5H_5$; n = 1, 2, 4; M = Fe, Co, Ni).

(b) Nonisothermal Low-Pressure Cold-Wall Conditions. The presence of either inert (N_2) or reactive (H_2) carrier gasses or a H_2/N_2 gas mixture and non isothermal conditions (vertical cold-wall reactor, Figure 2b) did not significantly change the properties of the obtained films (Figure 3a and Table 1b).

Analysis of the Thin-Film Composition, Purity. Table 1a,b shows the analytical composition of some representative examples of NiIn films grown from **1** under various conditions.

(a) Isothermal Vacuum Hot-Wall Conditions. The AES survey spectra and depth profiles (Figures 5 and 6) show levels of C and O below 5 atom % throughout the bulk of the films. N was not detected by AES. Elemental analysis obtained from combustion and AAS of 50−60 mg samples of thin film materials matches with the AES and EDX (metal content) values showing

(39) Staring, E. G. J.; Meeks, G. J. B. M. *J. Am. Chem. Soc.* **1989**, *111*, 7648.
(40) Hampden-Smith, M.; Kodas, T. In *The Chemistry of Metals CVD*; Verlag Chemie: Weinheim, 1994; pp 240−296.
(41) Glass, J. A. J.; Kehr, S. S.; Spencer, J. T. *Chem. Mater.* **1992**, *4*, 530.
(42) Fischer, R. A.; Priermeier, T.; Scherer, W. *J. Organomet. Chem.* **1993**, *459*, 65.
(43) Fischer, R. A.; Priermeier, T. *Organometallics* **1994**, *13*, 4306.
(44) Fischer, R. A.; Miehr, A.; Schulte, M. *Adv. Mater.* **1995**, *7*, 58.
(45) Steigerwald, M. L. *Chem. Mater.* **1989**, *1*, 52.
(46) Stuczynski, S. M.; Kwon, Y.-U.; Steigerwald, M. L. *J. Organomet. Chem.* **1993**, *449*, 167.
(47) Norman, N. C., personal communication, 1992.
(48) Skinner, H. A.; Connor, J. A. In *Molecular Structure and Energetics*; Liebman, J. F., Greenberg, A., Eds.; Verlag Chemie: Weinheim, 1987; Vol. 2, p 233.
(49) Colinet, C.; Bessoud, A.; Pasturel, A. *Z. Metallkde.* **1986**, *77*, 798.
(50) (a) Köster, W.; Horn, E. *Z. Metallkde.* **1952**, *43*, 333. (b) Dasarathy, C. *Z. Metallkde.* **1968**, *59*, 829. (c) Schwöbel, J.-D.; Stadelmeier, H. H. *Z. Metallkde.* **1970**, *61*, 342.

Scheme 1

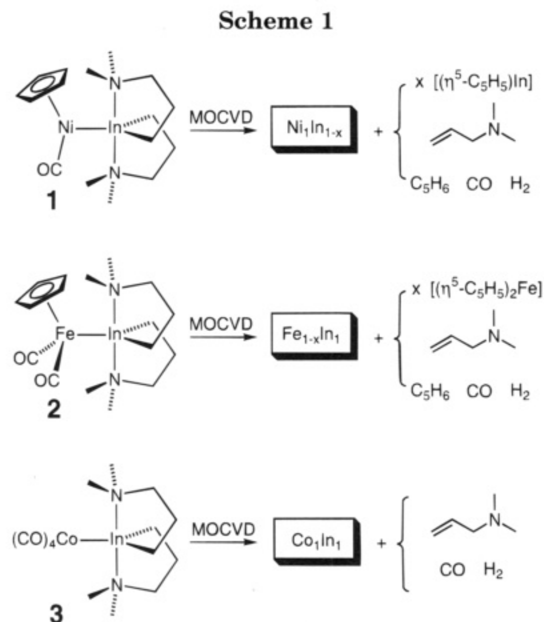

as well rather low contents of C, H, and O (N was not detected). The calculated C/H ratios of roughly 3 indicate that carbon impurities are likely to be graphitic or hydrocarbons but not essentially carbidic (line profiles by AES, XPS). Whether the residual C content originates from the CO ligand or from the cyclopentadienyl ligand is not absolutely clear. The 3-dimethylamino substituent at the indium center however seems not to be involved. This is indicated by comparison of the NiIn films grown from **1** with CoIn films grown from the related precursor $(CO)_4Co-In[(CH_2)_3NMe_2]_2$ (**3**), which does not contain the cyclopentadienyl group but the same indium fragment. CoIn films grown from **3** are essentially free of C and O (<0.5 at. %) within the accuracy of the AES method (confirmed by SIMS). The same is true for CoAs thin films grown from $(CO)_4Co-As[\eta^2-(^tBuNCH_2CH_2N^tBu)]$ (less than 1 at. % of C and O) compared with NiAs thin films grown from $(\eta^5-C_5H_5)(CO)Ni-As[\eta^2-(^tBuNCH_2CH_2N^tBu)]$ (3–6 at. % C).[51] It seems reasonable to identify the cyclopentadienyl ligand as the source of residual carbon impurities. Additionally, the low but detectable oxygen level could have other reasons than dissociative chemisorption of the CO ligand. The precursor **1** is rather moisture sensitive, which could result in a small contamination with oxygen containing products. They also may be volatile and decompose during MOCVD. However, a rigorous exclusion of oxygen and moisture was not possible due to lack of appropriate instrumentation and apparatus (e.g., a glovebox connected to the CVD apparatus to allow clean transfer of precursors and coated substrates and the use of glassware and O-ring seals to build parts of the reactor system). The analysis of the background gases by mass spectrometry showed partial pressures of $\sim 10^{-7}$ Torr for H_2O and $\sim 10^{-8}$ Torr for O_2 at a total base pressure of $\sim 10^{-6}$ Torr at the reaction zone. From these numbers it may be estimated,[52] that under the conditions of the MOCVD experiment at typical growth rates of roughly one monolayer per second (Table 1a), the expected level of oxygen incorporation caused by background impurities should be in the range of 1–2 at. % in our cases. This

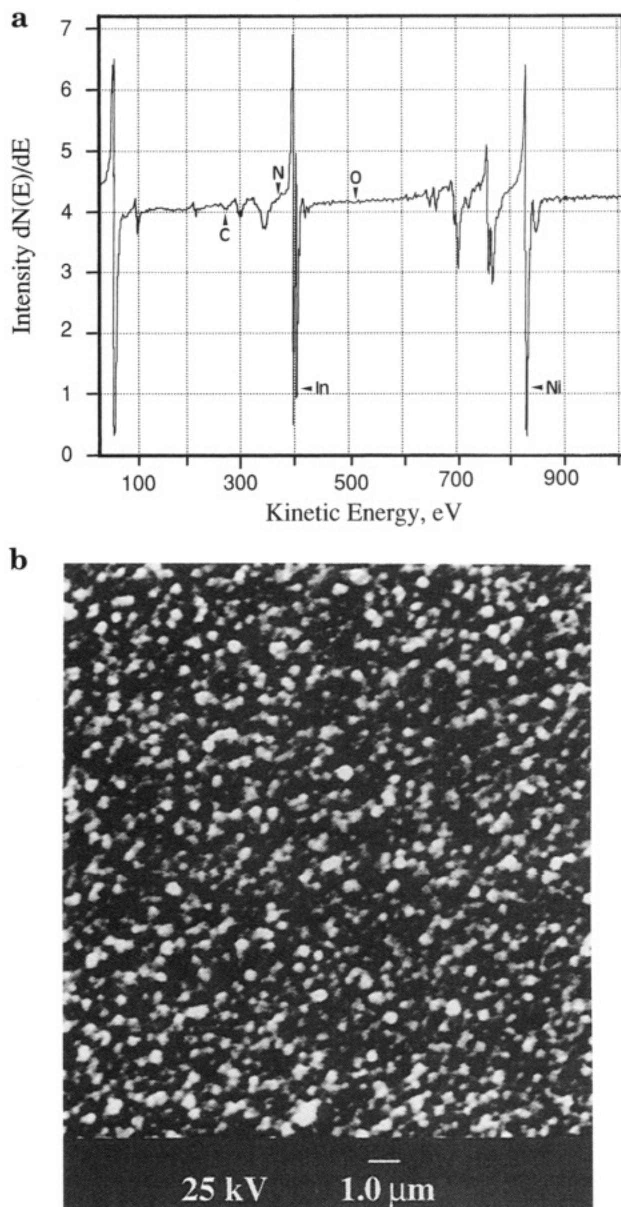

Figure 5. (a, top) Auger survey spectrum of film 16 (of Table 1b, cold-wall conditions) after 2 min of argon ion sputtering. Impurities of C, N, and O are close to the detection limit of the method. (b, bottom) The corresponding SEM image of the film.

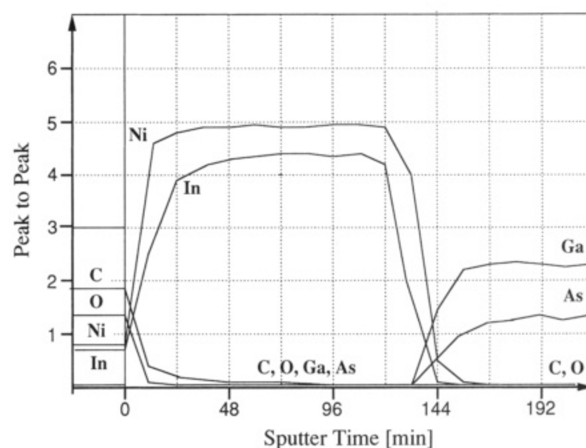

Figure 6. AUGER depth profile of film 4 (of Table 1a, hot-wall conditions) grown on a GaAs slide.

(51) (a) Herrmann, W. A.; Fischer, R. A.; Klingan, F. R.; Miehr, A. *Appl. Phys. Lett.*, in press. (b) Klingan, F. R. Ph.D. Thesis, Techn. Univ. Muenchen, 1995.

(52) Murarka, S. P. *Metallization, Theory and Applications*; Butterworth-Heinemann: Stoneham, 1993; pp 111–113.

level is quite close to the measured impurity levels of the best films. The high surface contaminations of C and O are most likely caused by the hydrolysis of condensed and not completely fragmented precursor molecules after cooling the reactor and subsequent transfer and handling of the coated substrates in air.

(b) Nonisothermal Low-Pressure Cold-Wall Conditions. The change from isothermal to nonisothermal conditions and the presence of inert carrier gases (N_2) and somewhat higher pressures around 0.1 Torr had no significant influence on the purity of the obtained NiIn films (Table 1b). But in the case of low substrate temperatures (200−250 °C) and hydrogen as reactive gas component, very pure Ni-rich Ni/In films were obtained, especially with respect to carbon. Kaesz et al. have pointed out that during MOCVD processes at low substrate temperatures hydrogen can efficiently reduce carbon contaminations if the growing metallic surface behaves as Fischer−Tropsch metal, e.g., as a hydrogenation catalyst.[53] This is the case for platinum and nickel but not for copper, for example. The surface of ϵ-NiIn is apparently not a very active hydrogenation catalyst (as can be seen from the dominating unsaturated organic byproducts), but rather Ni-rich Ni/In phases may be nonhomogeneous and may contain α-Ni, which can be deduced from the phase diagram.[54] This may account for the significant reduction in C content in these cases. This also agrees with the conjecture that the C content arises from the cyclopentadienyl ligands, because the clean decomposition of nickelocene also requires the presence of hydrogen at low temperatures to give 99% pure nickel.[55]

Structural Characterization. The Ni/In phase system is rather complex and was studied first by Hellner and Laves in 1947.[54] The literature is somewhat confusing and the Ni/In system has been reinvestigated several times. A comprehensive list of references was given by Andersson-Söderberg.[56] The low-temperature form of NiIn, which was called ϵ-NiIn by Hellner and Laves, has a very narrow range of homogeneity. Ni_3In, Ni_2In_3, and Ni_3In_7 have also narrow ranges. On the other hand, Ni_2In has a considerable homogeneity range from 61 to 67 at. % Ni. A monoclinic compound with composition $Ni_{13}In_9$ was identified by Ellner et al.[57] Figure 7 shows a powder X-ray diffraction diagram of a typical NiIn film grown on a GaAs(100) substrate at 350 (±20) °C at 10 (5) mTorr (experiment 4 of Table 1a). This particular film exhibited the best X-ray powder pattern in terms of intensity and signal-to-noise ratio compared to other films grown in this study. It was therefore chosen to confirm the structural and the phase identity of the deposited material. Table 2 shows the observed intensities and indexed reflections and *d* spacings. The measured values are in full agreement with the JCPDS-File reference no. 7-178 (except for some texture effects), which is based on Hellner's work in 1950.[58] The structure of ϵ-NiIn was

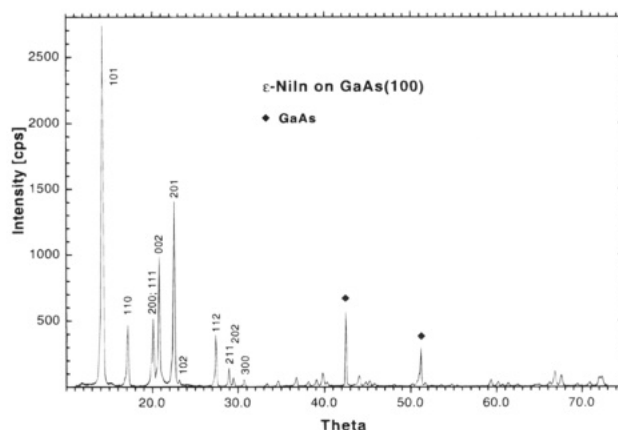

Figure 7. X-ray powder diffraction pattern of film 4 (see also Figure 6) on a GaAs slide recorded with an angle of incidence of 6°.

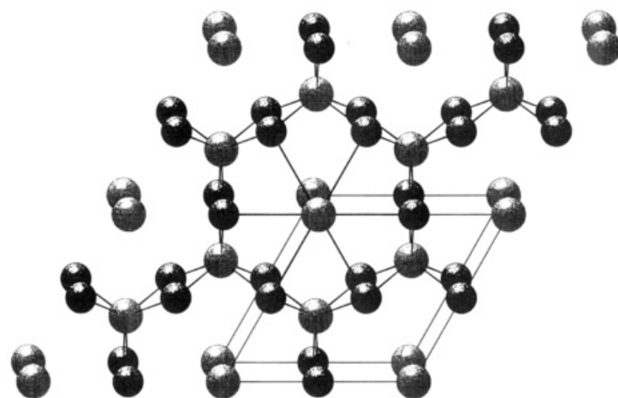

Figure 8. Crystal structure of ϵ-NiIn (Schakal representation; black, nickel atoms; grey, indium atoms).

proposed by Hellner and by Makarov[59] to be isotypical PtTl[60] and CoSn.[61] The obtained thin film thus consists of hexagonal ϵ-NiIn with the In atoms at the corners of the unit cell. Those indium atoms are surrounded by 6 Ni-atoms with a distance of 262 pm. The indium atoms at the positions ($^1/_3$ $^2/_3$ $^1/_2$) and ($^2/_3$ $^1/_3$ $^1/_2$), respectively are in the center of a prismatic hole and are surrounded by six nickel atoms with a Ni−In distance of 265 pm (Figure 8). Both Ni−In distances are within the range of the sum of the covalent radii and very similar to the Ni−In distance in the molecular species **1** which amounts to 259.8(1) pm. The lattice parameter given by Hellner[58] are incorrect (a = 453.6(5) pm and c = 434.4(5) pm). Using these values, the cell metric and the structure model, a density of 11.2 g cm^{-1} (Ni: ϱ = 8.9 g cm^{-3}; In: 7.3 g cm^{-3}) would result for hexagonal ϵ-NiIn ($Z = 3$, $V = 77.4$ Å^3, $M_{NiIn} = 173.5$ amu). However, the isostructural CoSn ($M_{CoSn} = 177.6$ amu) exhibits a much lower experimental and calculated density of 8.5 cm^{-3}. The density of various samples of the obtained NiIn thin film material was pycnometrically measured to amount 7.2(6) g cm^{-3}. A density of 8.3 g cm^{-3} was calculated from the lattice parameters for the ϵ-NiIn film. The density of the deposited film no. 4 was estimated to 8.1 (±0.9) g cm^{-3} (see also Experimental Part). The indexing of the measured reflections and a reindexing of the published values of Hellner unambiguously gave a =

(53) Zinn, A.; Niemer, B.; Kaesz, H. D. *Adv. Mater.* **1992**, *4*, 375.
(54) Hellner, E.; Laves, F. *Z. Naturforsch. A* **1947**, *2*, 177.
(55) Kaplin, Y. A.; Belysheva, G. V.; Zhil'tsov, S. F.; Domrachev, G. A.; Chernyshova, L. S. *Zh. Obsh. Khim., Int. Ed. Engl.* **1980**, *50*, 100.
(56) Andersson-Söderberg, M. *J. Less-Common Met.* **1990**, *171*, 179.
(57) Ellner, M.; Bhan, S.; Schubert, K. *J. Less-Common Met.* **1969**, *19*, 245.
(58) Hellner, E. *Z. Metallkde.* **1950**, *41*, 401.
(59) Makarov, E. S. *Izv. Akad. Nauk. S.S.S.R., Ser. Khim.* **1943**, 264.
(60) Zintl, A.; Harder, A. *Z. Elektrochem. Angew. Phys. Chem.* **1935**, 767.
(61) Nial, O. *Z. Anorg. Chem.* **1938**, *238*, 287.

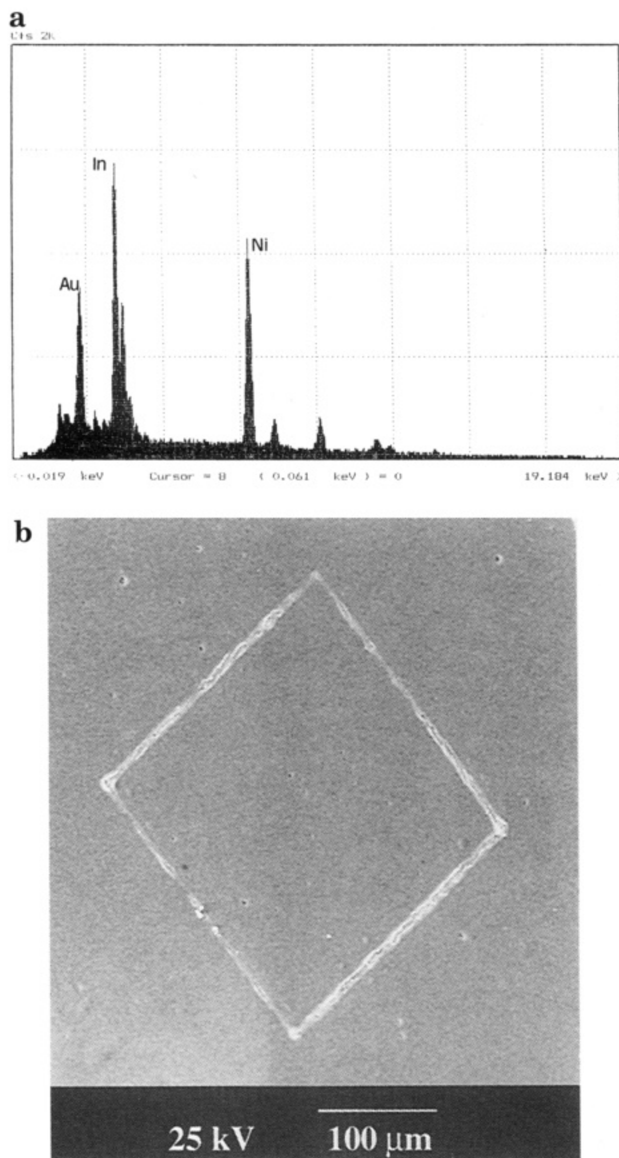

Figure 9. (a, top) Representative EDX-spectrum of a NiIn microstructure grown by direct laser writing on an alumina substrate. (b, bottom) SEM image of the structure. The sample was coated with a thin gold film by sputtering prior to the SEM-EDX investigations.

524.37(5) pm and $c = 435.09(5)$ pm as the correct lattice parameters. This is now in full agreement with the values given by Andersson-Söderberg and Makarov. The lattice parameters for the isotypical CoSn ($a = 526.8$ pm, $c = 424.9$ pm) are similar. The classification of ϵ-NiIn as an example for a NiAs phase by Best and Gödecke[62] is not possible on the basis of the cell parameters and appears to be confused with Brand's work on Ni_2In which exhibits a filled NiAs type structure.[63] The high signal-to-noise ratio, the low background noise, the agreement of calculated and measured density as well as the absence of other reflections than those of ϵ-NiIn indicate the obtained thin film no. 4 to be a phase-pure material. Similar X-ray powder patterns were obtained for other stoichiometric NiIn films grown on silicon, quartz and borosilicate glass.

Whether or not ϵ-NiIn or other Ni/In alloys may be chemically inert against a GaAs or a InP surface is still a matter of ongoing investigations. The hexagonal

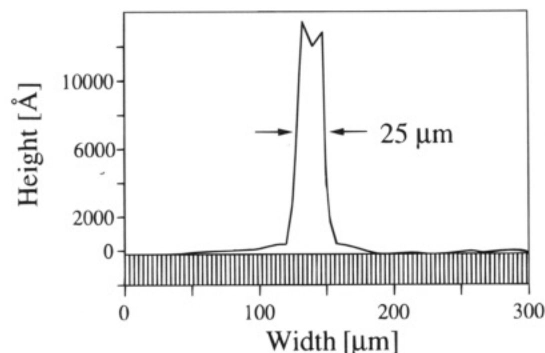

Figure 10. Line profile of the NiIn microstructure of Figure 9.

lattice structure of ϵ-NiIn clearly rules out a simple epitaxial relationship with GaAs or InP, as it is the case for the cubic β-CoGa[8] on GaAs. Our first NiIn films grown on InP substrates were surprisingly less crystalline than those grown on quartz or GaAs. We are currently trying to grow good-quality NiIn on InP from **1** and to investigate the thermal stability of those materials.

(B) Plasma-Enhanced MOCVD Experiments. Plasma-enhanced MOCVD experiments were also conducted using the apparatus of Figure 2b. However, the selectivity of the precursor decomposition was dramatically lower in these cases. The depositions were carried out at 300 °C at a plasma power of 40−60 W and with N_2 and a N_2/H_2 mixture as carrier gases. The obtained depositions (*not* included in Table 1a,b) showed very high levels of C and N (17−23 at. %) and low levels of Ni (11−16 at. %) and In (24−34 at. %). Apparently, plasma polymerization was the dominating process under our conditions. These findings are not at all surprising. The precursor **1** was designed to be thermally as fragile as possible while still exhibiting a comparably high volatily combined with an acceptable long-term stability at elevated temperatures. Plasma chemistry is a high-energy process, and one can anticipate, that the selectivity of the decomposition chemistry of **1** has to be lower. The poor quality of the films and the loss of stoichiometry control indicate, that compared with purely thermal conditions a very different decomposition chemistry of **1** is important under plasma conditions. The electron impact mass spectra of **1** (70 eV) show predominant fragmentation of the Ni−In bond into $[(\eta^5\text{-}C_5H_5)(CO)Ni^-]$ (m/z = 151, 100% rel. int.; negative ions) and $[In[(CH_2)_3N(CH_3)_2]_2^+]$ (m/z = 287, 100% rel. int.; positive ions). It is quite likely that the Ni−In bond is immediately ruptured under plasma conditions and the fragments may then undergo undesired predeposition gas-phase chemistry. For plasma applications, precursor **1** is clearly a bad choice.

(C) Photothermic Laser Direct Writing. Laser-induced pyrolytic direct writing of metallic microstructures using organometallic precursors has been described for various systems including copper,[64] gold,[33] platinum,[65] and aluminum.[66] To our knowledge, there is not report in the literature on direct laser writing of binary metallic alloys from single sources. Figure 10

(62) Best, K. J.; Gödecke, T. *Z. Metallkde.* **1969**, *60*, 659.
(63) Brand, P. *Z. Anorg. Allg. Chem.* **1967**, *353*, 270.
(64) Houle, F. A.; Jones, C. R.; Baum, T.; Pico, C.; Kovac, C. A. *Appl. Phys. Lett.* **1985**, *46*, 204−207.
(65) Koplitz, L. V.; Shuh, D. K.; Chen, Y. J.; Williams, R. S.; Zink, J. I. *Appl. Phys. Lett.* **1988**, *53*, 1705−1707.
(66) Baum, T. H.; Larson, C. E.; Jackson, R. L. *Appl. Phys. Lett.* **1989**, *55*, 1264−1266.

shows a SEM image of a Ni/In microstructure on an alumina substrate, which was grown by direct laser writing using the precursor **1**. The structure proved to be uniform with respect to the Ni/In composition. A representative EDX spectrum is also given in Figure 9 exhibiting a Ni/In ratio close to 1. This preservation of the stoichiometry of the metals was as expected, since the local temperatures, which are achieved during the laser deposition, are known to be relatively high.[67] Under our conditions, the spot temperature was surely greater than 350 °C, which was the minimum substrate temperature to achieve stoichiometric NiIn films under isothermal hot-wall conditions. The calculated deposition rates are on the order of 10^3 Å s^{-1}. The line profile (Figure 10) of the structure shows the "volcano type" pattern which is typical for high intensity.[67] The precursor compound **1** is transparent in the region of the wavelength of the laser (488 nm). Also, **1** shows no photochemistry in solution upon prolonged irradiation with a mercury lamp (254 nm). It is therefore, reasonable to rule out photochemical fragmentation processes of **1** during the deposition. Consequently, the properties of the obtained thin film microstructures of NiIn are very similar to the materials grown by conventional thermal MOCVD.

Conclusion

The successful growth of phase-pure ϵ-NiIn thin films from a volatile organometallic single-molecule source demonstrates for the first time that rather pure indium-containing mixed-metal thin films can be derived by simple MOCVD techniques. The study of the decomposition chemistry of **1** under isothermal vacuum conditions without carrier gases and under nonisothermal low-pressure conditions with carrier gases showed, that above a substrate temperature of 350 °C, the metal stoichiometry of the precursor is retained in the deposited alloy. Rather pure Ni-rich Ni/In films can be grown at low temperatures (250 °C) in the presence of hydrogen in a cold-wall reactor. The possibility of growing microstructures of binary alloys from single sources by direct laser writing was demonstrated. One inherent disadvantage of single source precursors is often their comparably low vapor pressure which may lead to rather low growth rates. The vapor pressure of **1** is sufficiently high at 80−90 °C (~0.1 Torr) to allow reasonable growth rates of 1−3 Å s^{-1}. The thermal analysis showed that the compound exhibits a good long term stability at the conditions of its vaporization. This precursor may thus be interesting for the deposition of metallic contacts to indium-containing III/V semiconductors (InP, InGaAs) by low-pressure MOCVD or CBE techniques. To serve as a stable metal/III−V semiconductor heterostructure, the metallic film should be chemically inert against the III/V−semiconductor surface. And in addition, the film should grow epitaxially. Both aspects have still to be investigated for the system NiIn/InP and NiIn/(In)GaAs. However, the results reported here may represent a good basis for these further studies, at least.

Acknowledgment. This work was supported by the Deutsche Forschungsgemeinschaft (Grant No. Fi 502/2-1 and 2-2) the Fonds der Chemischen Industrie, the Friedrich Schiedel Foundation, and the BMFT (Grant No. 13N615917, MPI Göttingen). The authors also wish to acknowledge the valuable contributions of Dr. W. Scherer to the structural part (i.e., the accurate measurements of the X-ray diffraction patterns and the conformation of the phase identity of the ϵ-NiIn films).

CM950111A

(67) Houle, F. A.; Baum, T. H.; Moylan, C. R. In *Laser Chemical Processing for Microelectronics*; Ibbs, K. G., Osgood, R. M., Eds.; Cambridge University: Cambridge, 1989; p 25.